Am J Cancer Res 2023;13(12):6090-6098
www.ajcr.us /ISSN:2156-6976/ajcr0151596

Original Article

Risk prediction of poor wound healing in patients with thoracoscopic lung cancer resection with drainage tube

Yuguo Chen[1,2*], Congying Ji[1,2*], Chuan Huang[2,3], Ting Zhou[2,3], Xia Wang[2,4]

[1]Dressing Room of Surgical Outpatient Department, Beijing Hospital, National Center of Gerontology, Beijing 100730, China; [2]Institute of Geriatric Medicine, Chinese Academy of Medical Sciences, Beijing 100021, China; [3]Department of Thoracic Surgery, Beijing Hospital, National Center of Gerontology, Beijing 100730, China; [4]Nursing Department, Beijing Hospital, National Center of Gerontology, Beijing 100730, China. [*]Equal contributors and co-first authors.

Received June 5, 2023; Accepted September 12, 2023; Epub December 15, 2023; Published December 30, 2023

Abstract: This work established a risk prediction (RP) model for poor wound healing (PWH) in patients with thoracoscopic lung cancer (LC) resection (TLCR) after drainage tube placement to explore its application effect. 359 patients with TLCR were categorized into a good wound healing group (GWH group, 275 cases) and a poor wound healing group (PWH group, 84 cases) based on incision healing condition. The independent prediction risk factors (IPRFs) of PWH were analyzed and a RP model was constructed. 70% of the patients were classified as the model group (Mod group) and 30% were in the validation group (Val group). Resolution of the RP model was evaluated by the area under receiver operating characteristic (ROC) curve (AUC). The Hosmer-Lemeshow goodness of fit (HLGF) test was employed to evaluate the calibration of RP model. Results from the multivariate logistic regression analysis (MLRA) showed that age, preoperative albumin levels, diabetes history, dressing change frequency, and type of wound cleaning fluid were independent risk factors (IRFs) for postoperative PWH ($P<0.05$). In the Mod group, AUC=0.758 ($P<0.05$, 95% CI=0.712-0.806), and HLGF test showed $P=0.493$. In the Val group, AUC=0.783 ($P<0.05$, 95% CI=0.675-0.834), and HLGF test showed $P=0.189$. In conclusion, the constructed model was convenient, feasible, and demonstrates good predictive performance for postoperative incision healing issue, holding practical value and applicability.

Keywords: Lung cancer, thoracoscopy, poor wound healing, risk factors, risk prediction model

Introduction

Lung cancer (LC) is a prevalent and aggressive tumor worldwide, showing a malignant nature. According to the latest data from the International Agency for Research on Cancer of the World Health Organization (WHO) in 2020, LC is the most newly diagnosed cancer in China [1]. The global death toll from LC stands at approximately 1.8 million, ranking it as the leading cause of cancer-related deaths. The new cases of LC accounted for about 17.9% of the total number of new cancers, and the deaths of LC accounted for 23.8% of all cancer deaths. With China stepping into an aging society, increased social industrialization, the high smoking rate and other factors, the incidence and mortality of LC remain challenging to improve [2]. With the popularization of low-dose computed tomography (CT) screening, more LC patients are being detected at early stages. The ways of pre-treatment of LC include surgery [3], immunotherapy [4], chemoradiotherapy [5], and targeted therapy [6], but surgical resection remains the primary option. Recently, thoracoscopic minimally invasive technology has witnessed continuous innovation and development, offering numerous advantages, such as smaller incision, faster recovery, fewer postoperative complications, and less pain. Moreover, for patients with early non-small cell LC, precise dissection of lung segments and corresponding lymph node dissection can be performed [7]. Consequently, many LC surgeries abandon the original thoracotomy and choose the current thoracoscopic LC radical operation, which has become a routine operation in most hospitals.

Advancements in surgery and anesthesia have reduced the incidence of adverse outcomes after LC. However, in thoracoscopic radical LC operations, the prolonged use of drainage tubes and individual patient factors can reduce the body's resistance, increasing the risk of bacterial infiltration into the incision [8]. Additionally, the presence of drainage tube depresses the incision and friction for a long time, affecting blood supply to the local incision, resulting in hypoxia of tissue cells and further increasing the possibility of bacterial invasion, leading to noticeable symptoms such as incision redness and swelling of the incision, darkening of skin edge, skin edge necrosis, fat liquification, and poor healing of pus [9, 10]. These complications not only prolong the length of hospital stay, affects the surgical effect and increases the risk of complications, but also directly affects the surgical quality, postoperative rehabilitation and prognostic effect of patients [11]. Poor wound healing (PWH) not only delays the patient's hospital stay and increases the patient's economic burden, but also causes the patient pain and increases doctor-patient conflict [12]. About 600 cases of LC thoracoscopic surgeries are performed annually in our hospital. After discharge, patients underwent dressing changes and stitches were removed in the dressing room. Nearly 60-70% of patients with closed drainage incision experienced wound healing problems, requiring suture or dressing change, which was similar to a foreign study [13]. Although some researchers have only analyzed the wound healing of closed thoracic drainage and related factors, there is a lack of comprehensive studies encompassing specific diseases and surgical methods [14]. There have been no studies on PWH after thoracoscopic closed drainage in LC patients.

In this work, PWH factors of patients with LC after thoracoscopic closed drainage were analyzed, and a prediction model was established and verified through risk factors. It was hoped that the prediction model after verification can be popularized in the industry and used for drainage incision healing risk prediction (RP) to raise the attention of colleagues to the drainage tube incision healing and reduce the incidence of PWH.

Materials and methods

Ethics approval

This study was approved by the ethics committee of the Beijing Hospital of Chinese Academy of Medical Sciences (Approval number: 2022BJYYEC-057-01). All the experiments of this study were conducted in accordance to the relevant guidelines and regulations or in accordance to the Declaration of Helsinki. Informed consent was obtained from all subjects involved in the study.

Research objects

In a retrospective analysis from January 1, 2022, to December 31, 2022, 359 patients who underwent thoracoscopic lung cancer resection (TLCR) at Beijing Hospital had their dressings changed and sutures removed in the operating room. Patients were rolled into a good wound healing group (GWH group, 275 cases) and a PWH group (84 cases) according to the wound healing condition. The patients were enrolled if they met all the following conditions: ① age above 18 years old; ② undergoing TLCR in thoracic surgery department of our hospital without conversion to thoracotomy; ③ with diabetes, hypertension, hyperlipidemia, and other underlying diseases which were controlled within the range of surgical indications during the perioperative period; and ④ with complete pathological and clinical data. They had to be excluded from this work if they had any of below conditions: ① patients who could not take care of themselves; ② patients with senile dementia and mental retardation; ③ those with other life-threatening diseases, such as serious cardiovascular and cerebrovascular diseases; ④ patients with previous thoracic surgery; and ⑤ those without pulmonary infections before operation.

Diagnostic criteria and definitions

PWH criteria for surgical treatment were as follows. In this work, the diagnostic criteria for PWH after drainage tube in the chest and abdominal cavity were according to the Diagnostic Criteria for Nosoconial Infection (Trial) prescribed by the Ministry of Health. Grade B (local wound redness, induration, hematoma, and exudation) and grade C (purulent wound) meant PWH.

BMI classification was determined according to Chinese Health Industry Standard: Adult Body Weight Measurement (WS/T428-2013). BMI<18.5 kg/m^2, 18.5 kg/m^2<BMI<24.0 kg/m^2, 28.0 kg/m^2>BMI>24.0 kg/m^2, and BMI>28 kg/m^2 were considered to be underweight, normal weight, overweight, and obese, respectively.

Prognostic nutritional index (PNI) was calculated by serum albumin count (g/L) + 5 * lymphocyte count (10^9/L).

The normal Hb ranges for men and women were 120 g/L and 110 g/L, respectively; and anemia was defined if the Hb value was below the normal range.

Postoperative wound condition

The postoperative wound condition was observed ① during the hospitalization (the first day after surgery, at extubation, and before discharge) and ② after discharge (dressing was changed once on the 3rd, 7th, and 11th day after discharge, to three days before the drainage tube removal).

Observation indicators

Before surgery, gender, age, BMI, preoperative albumin, smoking history, past medical history (diabetes, hypertension, and immune system diseases), hormone and immunosuppressive drug history, and preoperative chemoradiotherapy were observed and compared.

During the surgery, operation time, resection range, surgical side, intraoperative bleeding, and the number of suture needles in the drainage tube incision were observed.

After the surgery, drainage volume, pathological stage, extubation time, postoperative complications, Visual Analogue Scale/Score (VAS), dressing change frequency, type of wound cleaning fluid, wound condition during dressing change, suture removal time, and wound healing after suture removal were observed and compared.

Calculation of sample size

According to the rough estimation method, the sample size of 29 variables was 5-10 times larger than that of variables, and the sample size was 145-290 cases, who were selected for the initial estimate. 70% was randomly selected for modeling and 30% for model inspection.

Statistical analysis

SPSS 24.0 was utilized to process the data. Variables conforming to the normal distribution were displayed with mean ± standard deviation ($\overline{x}$ + s), otherwise the data were described by median and quartile. The correlation factors of PWH in closed drainage after TLCR were determined by single factor analysis, and the test method was X^2 test. Statistically significant variables identified by univariate analysis were undertaken as independent variables for MLRA, and variables with $P<0.05$ were IRFs. During the construction of RP model, the OR value (rounded) was applied to assign values to all factors entering the logistic regression equation, and the RP equation for postoperative AF complications in LC patients was established. The value corresponding to the maximum Yoden index was undertaken as the best diagnosis threshold. The AUC was utilized to evaluate the resolution of RP model. The calibration of RP was evaluated by HLGF, and $P>0.05$ indicated a good model fitting. During verification of the RP model, risk scores and total risk scores of each patient in Val group were calculated according to RP model equation, and AUC and HLGF were selected to evaluate postoperative PWH compliance and discriminant validity of patients in Val group LC.

Results

Patients

Among the patients enrolled herein, there were 155 (43.2%) males and 204 (56.8%) females, with an average age of (62.88 ± 10.48) years and an average BMI of (24.19 ± 3.34) kg/m^2. After surgical treatment, incision healing was normal in 275 (76.6%) patients (**Table 1**).

Single factor analysis of PWH

Among the patients enrolled, 275 patients had good postoperative wound healing and 84 patients had postoperative PWH. In patients in the GWH group, the mean age was (57.36 ± 9.94) years old, the operation time was (129.83 ± 27.46) min, the preoperative albumin was (42.73 ± 7.29) g/L, 35 cases (12.73%)

Table 1. General information of patients

Index	Number of cases	Value
Age (years)	359	62.88 ± 10.48
BMI (kg/m^2)	359	24.19 ± 3.34
Male	155	43.2%
Female	204	56.8%
Number of stitches (each)	359	1 (1, 1)
Albumin (g/L)	356	37 (35, 39)
Extubation time (min)	359	3 (3, 4)
Operation time (min)	358	130 (100, 170)
Past medical history		
Hypertension	161	44.8%
Diabetes	55	15.3
Diseases of immune system	55	15.3
Extubation time classification		
1~3 days after surgery	234	65.2
4 days after surgery	125	34.8
Clinical outcome		
Healing	275	76.6
Nonunion	84	23.4

had the previous diabetes history, the intraoperative blood loss (IBL) was (224.6 ± 113.7) mL, pathological stage, dressing change frequency, and type of wound cleaning fluid showed great differences with those in the PWH group (P<0.05) (**Table 2**).

Multivariate analysis of PWH

As can be observed from **Table 2**, age, operative time, pre-operative albumin level, previous diabetes history, resection scope, IBL, pathological stage, dressing change frequency, and type of wound cleaning fluid showed great differences with P<0.05. Therefore, MLRA was continued for these indicators, and the results revealed that, age, preoperative albumin, diabetes history, dressing change frequency, and type of wound cleaning fluid were the IRFs of postoperative PWH (P<0.05).

Construction of RP model for PWH

According to the MLRA results, each independent predictor was assigned according to the OR value (rounded to an integer), which was the risk score of this variable (**Table 3**). The prediction equation of postoperative PWH was as follows: 3 * old age + 7 * preoperative albumin + 7 * diabetes history + 1 * dressing change frequency + 4 * type of wound cleaning fluid. According to the RP model equation, the risk score of each variable of each research object was added to obtain the total risk score of each patient, with the lowest score being 0 and the highest being 22. ROC curve of postoperative PWH predicted by this model was drawn according to the total risk score, based on which it was concluded that the AUC=0.758 (P<0.05, 95% CI=0.712-0.806) (**Figure 1**). This indicated that this model had a good ability to predict the postoperative PWH. The results of Yoden index suggested that the optimal diagnostic threshold of this RP model was 13 points. The sensitivity and specificity of this truncation value were 80.4% and 71.3%, respectively. The HLGF test of the model showed that X^2=0.837, P=0.493>0.05, indicating that the calibration degree of the RP model was high and the model fit was good.

Verification of RP model for PWH

According to this RP model, the total risk value of each patient in the Val group was calculated, based on which the ROC curve of postoperative PWH of patients in the Val group was drawn. It revealed that AUC=0.783 (P<0.05, 95% CI=0.675-0.834) (**Figure 2**). The HLGF test of this model was conducted in Val group and revealed X^2=2.946 and P=0.189>0.05. It indicated that the calibration degree of the model was high, the fitting degree was good, and the RP model had a certain stability.

Discussion

LC is one of the major diseases threatening human health, and its morbidity and mortality rank the first among malignant tumors in rural and urban areas [15]. On the one hand, the incidence of lung cancer is on the rise due to the gradual increase in environmental pollution and an increase in the population of smokers [16]. On the other hand, as medical technology progresses and new technologies are applied, hospitals across the country are gradually adopting technologies such as fiberoptic bronchoscopy biopsy and alveolar lavage. Non-

Table 2. Univariate analysis of PWH risk factors

Indicators	GWH group (n=275)	PWH group (n=84)	X^2	*P*
Age (years old)*	57.36 ± 9.94	68.27 ± 7.33	7.164	0.007
BMI (kg/m^2)	24.07 ± 2.57	24.18 ± 2.62	0.937	0.209
Operation time (min)*	129.83 ± 27.46	138.77 ± 32.14	9.636	0.002
Gender			0.088	2.094
Male	121 (44%)	34 (40.48%)		
Female	154 (56%)	50 (59.52)		
Preoperative albumin (g/L)*	42.73 ± 7.29	31.52 ± 6.46	11.925	0.000
Smoking history (cases)	103 (37.45%)	32 (38.1%)	0.036	3.845
Past medical history				
Hypertension	103 (43.64%)	41 (48.81%)	0.268	0.579
Diabetes	35 (12.73%)	20 (23.81%)	8.734	0.004
Diseases of immune system	40 (14.55%)	14 (16.67%)	0.836	0.217
Preoperative treatment (cases)				
Hormone	22 (8%)	5 (5.95%)	3.928	0.124
Immunosuppressant	18 (6.55%)	5 (5.95%)	0.106	1.985
Chemoradiotherapy	27 (9.82%)	10 (11.9%)	0.463	0.501
Excision range (cases)*			9.073	0.014
Partial excision	201 (73.09%)	51 (60.71%)		
Lung lobes and above	74 (26.95%)	33 (39.29%)		
Surgical side (cases)			2.168	0.173
Left side	184 (66.91%)	55 (65.48%)		
Right side	91 (33.09%)	29 (34.52%)		
IBL (mL)*	224.6 ± 113.7	295.8 ± 106.6	10.782	0.001
Drainage volume (mL)	428.17 ± 139.5	413.8 ± 148.6	0.583	0.494
Number of stitches			3.382	0.975
<5	142 (51.64%)	47 (55.95%)		
5 or more	133 (48.36%)	37 (44.05%)		
Pathological stage (case)*			7.372	0.028
I~II	183 (66.55%)	45 (53.57%)		
III~IV	92 (33.45%)	39 (46.43%)		
Extraction time			4.219	0.136
1~3 days after surgery	177 (64.36%)	57 (67.86%)		
4 days after surgery	98 (35.64%)	27 (32.14%)		
Postoperative complications (cases)			4.283	0.133
Arrhythmology	23 (8.36%)	8 (9.52%)		
Pneumonia	28 (10.18%)	8 (9.52%)		
Atelectasis	14 (5.09%)	4 (4.76%)		
Pleural effusion	8 (2.91%)	1 (1.19%)		
Respiratory failure	17 (6.18%)	6 (7.14%)		
Postoperative VAS score	3.7 ± 1.8	3.9 ± 1.4		
Dressing change frequency*				
1 day/time	81 (29.45%)	38 (45.24%)	9.192	0.000
2~3 days/time	194 (70.55%)	46 (54.76%)		
Type of wound cleaning fluid*			7.781	0.008
Normal saline	118 (42.91%)	53 (63.1%)		
Antibiotic solution	157 (57.09%)	31 (36.9%)		
Removal time (d)	8.2 ± 1.6	8.5 ± 1.3	2.784	1.388

Note: * indicated an obvious difference with $P<0.05$.

Table 3. MLRA results of PWH

Influencing factors	β	S.E.	Wald	OR	P	95% CI	
						Upper limit	Lower limit
Old age	1.232	0.548	4.113	3.373	<0.05	1.006	9.521
Preoperative albumin	2.937	0.435	6.824	7.103	<0.05	6.938	3.268
Diabetes history	1.893	0.831	4.483	6.995	<0.01	1.204	10.748
Excision area	-0.005	0.057	0.017	0.984	0.838	0.913	1.635
Intraoperative blood loss	-0.596	0.749	0.836	0.738	0.491	2.147	0.397
Pathological stage	0.205	0.592	0.039	1.086	0.704	3.674	0.765
Dressing change frequency	-1.098	0.483	6.204	1.291	<0.05	0.639	0.003
Type of wound cleaning fluid	3.166	0.745	17.425	4.143	<0.01	5.474	8.627

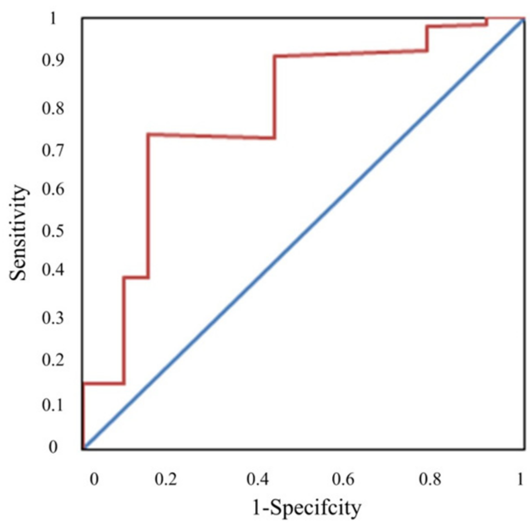

Figure 1. ROC curve in the Mod group.

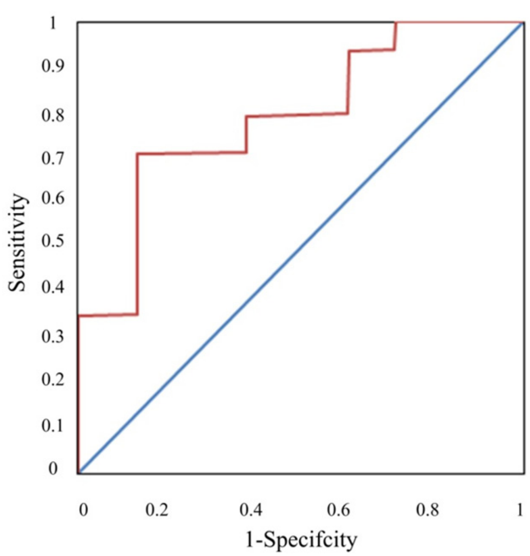

Figure 2. ROC curve in the Val group.

surgical procedures now allow for the accurate collection of lung lesion specimens and advance pathological diagnosis, thus improving the diagnosis rate of LC [17]. With the rapid development of thoracoscopic surgery, it has become the first choice of LC surgical treatment. Compared with traditional thoracotomy, thoracoscopic surgery shortens the length of hospital stay of patients, reduces the occurrence of postoperative complications, and improves the surgical effect [18]. Despite the necessity for drainage tubes after surgery to ensure full drainage of the residual cavity, some patients suffer from PWH, which has an adverse effect on the surgical effect [19]. In this work, factors related to drainage tube PWH after LC were analyzed, and the RP model of PWH was constructed to explore its predictive value in PWH of patients after LC.

Among the research indicators included in this work, age, operative time, preoperative albumin level, previous diabetes history, resection scope, IBL, pathological stage, dressing change frequency, and type of wound cleaning fluid demonstrated great differences with $P<0.05$. Further MLRA revealed that, age, preoperative albumin, diabetes history, dressing change frequency, and type of wound cleaning fluid were the IRFs of postoperative PWH ($P<0.05$). Muazama et al. (2022) [20] found that low levels of albumin and poor glycemic control prior to surgery were associated with delayed wound healing. Moreover, a previous study [21] has reported that age-related changes in the epidermis and dermis can alter the ability of skin to resist injury, possibly contributing to PWH in elderly patients. All of them are consistent with the results of this work. Finally, the RP model was constructed based on the obtained IPRFs of

PWH, with AUC=0.758 ($P<0.05$, 95% CI=0.712-0.806) and AUC=0.783 ($P<0.05$, 95% CI=0.675-0.834) in the Mod group and Val group, respectively, indicating that the prediction performance of this model is good. According to the Yoden index, the optimal diagnostic cut-off value of this RP model was 13 points, with corresponding sensitivity and specificity values of 80.4% and 71.3%, respectively. The HLGF test was conducted on patients in the Mod group and Val group, and their *P* values were 0.493 and 0.189, respectively, which were >0.05. It indicates that the model had a high calibration degree, a good fitting degree, and a high resolution. It is important to note that there are many genetic, biochemical, physiological, and epigenetic findings related to lung cancer [22-48].

In conclusion, the RP model of PWH constructed in this work could be valuable in clinical practice and served as a useful tool for medical staff to identify patients with high risk of PWH, enhancing their management to improve patient outcomes. However, the patients included herein were all provided by our institute, leading to potential selection bias. In addition, some indicators were too few to be included, such as the selection of postoperative complication indicators. To address these limitations, further large-sample and multi-center studies with longer follow-up periods are recommended. Such studies will strengthen model optimization and external validation to promote better clinical application of RP model and prognostic management of LC patients.

Conclusions

This work showed that age, preoperative albumin, diabetes history, dressing change frequency, and type of wound cleaning fluid were all IRFs of patients with postoperative PWH. Then, the RP model for PWH was successfully constructed and verified according to these variables. The results indicated that the model was convenient, feasible, and had good predictive performance. The results indicated that the model is convenient, feasible, and exhibits good predictive performance, making it valuable for practical applications. However, this work was subjected to a bias in sample selection, and some indicators were too few to be enrolled. If possible, it was necessary to conduct a large-sample and multi-center study for one-step optimization model in the future.

Acknowledgements

The research is supported by: National High Level Hospital Clinical Research Funding BJ-2021-218; National High Level Hospital Clinical Research Funding BJ-2019-165.

Disclosure of conflict of interest

None.

Abbreviations

RP, risk prediction; PWH, poor wound healing; LC, lung cancer; IPRFs, independent prediction risk factors; Mod group, model group; Val group, validation group; ROC, receiver operating characteristic; HLGF, The Hosmer-Lemeshow goodness of fit; MLRA, multivariate logistic regression analysis; IRFs, independent risk factors; WHO, World Health Organization; CT, computed tomography; TLCR, thoracoscopic lung cancer resection.

Address correspondence to: Xia Wang, Institute of Geriatric Medicine, Chinese Academy of Medical Sciences, Beijing 100021, China. Tel: +86-106-9155937; Fax: +86-1069155937; ORCID: 0000-0003-1993-2695; E-mail: xiawang980@mailfence.com; minshipu4400305264@163.com

References

[1] Lv D, He L, Guo L, Zhang X and He X. Acute kidney injury induced by immune checkpoint inhibitors in lung cancer patients. Discov Med 2022; 33: 137-141.

[2] Wang B, Zhang Z, Tang J, Tao H and Zhang Z. Correlation between SPARC, TGFβ1, endoglin and angiogenesis mechanism in lung cancer. J Biol Regul Homeost Agents 2018; 32: 1525-1531.

[3] Tong C, Miao Q, Zheng J and Wu J. A novel nomogram for predicting the decision to delayed extubation after thoracoscopic lung cancer surgery. Ann Med 2023; 55: 800-807.

[4] Reck M, Remon J and Hellmann MD. First-line immunotherapy for non-small-cell lung cancer. J Clin Oncol 2022; 40: 586-597.

[5] Wang SF, Mao NQ, Zhao WH and Pan XB. Postoperative radiotherapy in pIIIA-N2 non-small cell lung cancer after complete resection and adjuvant chemotherapy: a meta-analysis. Medicine (Baltimore) 2022; 101: e29550.

[6] Osmani L, Askin F, Gabrielson E and Li QK. Current WHO guidelines and the critical role of immunohistochemical markers in the subclassification of non-small cell lung carcinoma (NSCLC): moving from targeted therapy to immunotherapy. Semin Cancer Biol 2018; 52: 103-109.

[7] Davakis S, Charalabopoulos A, Kyros E, Sakarellos P, Tsourouflis G, Dimitroulis D and Nikiteas N. Minimally invasive transcervical esophagectomy with mediastinal lymphadenectomy for cancer. A comparison with standardized techniques. Anticancer Res 2022; 42: 675-680.

[8] Akiyama T, Yano M, Numanami H, Yamaji M, Taguchi R, Furuta C, Kitagawa Y, Imazu R and Haniuda M. Surgical site infection at chest tube drainage site following pulmonary resection for malignant lesions. J Thorac Dis 2021; 13: 1445-1454.

[9] Fu R, Zhang JT, Dong S, Chen Y, Zhang C, Tang WF, Xia J, Nie Q and Zhong WZ. Drainage tube hole suture improvement: removal-free stitches. Thorac Cancer 2019; 10: 1827-1833.

[10] Dziri C, Dougaz W, Khalfallah M, Samaali I, Nouira R and Fingerhut A; Co-investigators. Omentoplasty decreases deep organ space surgical site infection compared with external tube drainage after conservative surgery for hepatic cystic echinococcosis: meta-analysis with a meta-regression. J Visc Surg 2022; 159: 89-97.

[11] Majumdar M, Lella S, Hall RP, Sumetsky N, Waller HD, McElroy I, Sumpio B, Feldman ZM, Kim Y, DeCarlo C, Warner M, Nuzzolo K, Kirshkaln A and Dua A. Utilization of thromboelastography with platelet mapping to predict infection and poor wound healing in postoperative vascular patients. Ann Vasc Surg 2022; 87: 213-224.

[12] Liang X, Han-Xin Z, Chang-E J, Chao W, Juan H and Guo-Quan G. Subcutaneous suture can accelerate wound healing of lower midline incision: a randomized controlled trial. Am Surg 2015; 81: 23-30.

[13] Newman JM, Siqueira MBP, Klika AK, Molloy RM, Barsoum WK and Higuera CA. Use of closed incisional negative pressure wound therapy after revision total hip and knee arthroplasty in patients at high risk for infection: a prospective, randomized clinical trial. J Arthroplasty 2019; 34: 554-559, e1.

[14] Xu Y, Guo Z, Huang J, Liu R, Ning J, Feng L and Tan Q. Simple continuous suture to strengthen the closure of intra-muscle used in the removal of uni-portal video-assisted thoracoscopic surgery thoracic drainage tube. Ann Transl Med 2019; 7: 764.

[15] Xiang Y, Song J, Yan Y and Xia H. Status survey of sleep quality of lung cancer patients and analysis of influencing factors. Acta Medica Mediterranea 2022; 38: 3409-3413.

[16] Alexander M, Kim SY and Cheng H. Update 2020: management of non-small cell lung cancer. Lung 2020; 198: 897-907.

[17] National Lung Screening Trial Research Team. Lung cancer incidence and mortality with extended follow-up in the national lung screening trial. J Thorac Oncol 2019; 14: 1732-1742.

[18] Mun M, Nakao M, Matsuura Y, Ichinose J, Nakagawa K and Okumura S. Video-assisted thoracoscopic surgery lobectomy for non-small cell lung cancer. Gen Thorac Cardiovasc Surg 2018; 66: 626-631.

[19] Yang S, Wu Q, Wang Q and Lv F. Magnetic resonance imaging under image enhancement algorithm to analyze the clinical value of placement of drainage tube on incision healing after hepatobiliary surgery. Comput Math Methods Med 2022; 2022: 9269695.

[20] Zaffar M, Afreen A, Waseem M and Ahmed Z. Effect of nutritional status on wound healing after coronary artery bypass graft (CABG) surgery. J Pak Med Assoc 2022; 72: 860-865.

[21] Bonifant H and Holloway S. A review of the effects of ageing on skin integrity and wound healing. Br J Community Nurs 2019; 24: S28-S33.

[22] Li C, Lu H, Jiang X, Guo X, Zhong H and Li H. Network pharmacology study of citrus reticulata and pinellia ternata in the treatment of non-small cell lung cancer. Cell Mol Biol (Noisy-le-grand) 2022; 67: 10-17.

[23] Lv K, Yang X, Li Z, Ma C and Hong Q. Circulating tumor DNA detection in peripheral blood in postoperative efficacy evaluation and recurrence risk prediction of lung cancer. Cell Mol Biol (Noisy-le-grand) 2022; 67: 51-56.

[24] Çetin İ and Topçul M. Antiproliferative effects of EGFR inhibitor cetuximab and PARP inhibitor combination on non-small cell lung cancer cell line A549 and cervical cancer cell line HeLa. Cell Mol Biol (Noisy-le-grand) 2022; 68: 47-51.

[25] Bajrai LH, Sohrab SS, Khalid M, Kamal MA and Azhar EI. Molecular interaction of cryptophycin 52 with caspase 8 for the management of lung cancer during coronavirus outbreak: a computational study. Cell Mol Biol (Noisy-le-grand) 2022; 68: 31-35.

[26] Zhang Y, Lu N, Pu S and Mu K. Significance of screening sensitive methylation sites using whole-genome sequencing in early diagnosis of non-small cell lung cancer. Cell Mol Biol (Noisy-le-grand) 2022; 67: 218-226.

[27] Shan S, Bao Q, Ma G, Yao Y, Xiong J and You J. Human antigen R affects the migration and invasion of human lung cancer A549 cells via

regulating E-cadherin suppressor snail. Cell Mol Biol (Noisy-le-grand) 2022; 68: 9-16.
[28] Feng Y, Wang W and Liu C. Effect of solanum lyratum polysaccharide on malignant behaviors of lung cancer cells by regulating the circ_UHRF1/miR-513b-5p axis. Cell Mol Biol (Noisy-le-grand) 2022; 67: 191-199.
[29] Lin J, Xu F, Zhang C and Wu B. The effect of some trace elements on the expression of telomerase gene in lung cancer. Cell Mol Biol (Noisy-le-grand) 2022; 68: 86-90.
[30] Pandey P, Khan F, Chauhan P, Upadhyay TK, Bardakci F, Alam MJ, Almuzaini N, Abdalla RAH, Singh SK and Saeed M. Elucidation of the inhibitory potential of flavonoids against PKP1 protein in non-small cell lung cancer. Cell Mol Biol (Noisy-le-grand) 2022; 68: 90-6.
[31] Avşar EN, Çetin İ and Topçul M. An overview of the effect of the Wnt signaling pathway in lung cancer. Cell Mol Biol (Noisy-le-grand) 2022; 68: 41-46.
[32] Gu M, Chen Z, Xiong H, Liu K, Ye Z and You Q. Role and clinical significance of LncRNA16 in the malignant proliferation of lung cancer cells. Cell Mol Biol (Noisy-le-grand) 2022; 68: 177-181.
[33] Yang T. Expression profile of IL-17 in lung tissues of patients with lung cancer and COPD and clinical significance. Cell Mol Biol (Noisy-le-grand) 2022; 68: 135-139.
[34] Xu G, Yu B, Wang R, Jiang J, Wen F and Shi X. Astragalin flavonoid inhibits proliferation in human lung carcinoma cells mediated via induction of caspase-dependent intrinsic pathway, ROS production, cell migration and invasion inhibition and targeting JAK/STAT signalling pathway. Cell Mol Biol (Noisy-le-grand) 2021; 67: 44-49.
[35] Ramazi S, Daddzadi M, Sahafnejad Z and Allahverdi A. Epigenetic regulation in lung cancer. MedComm (2020) 2023; 4: e401.
[36] Hu W, Hu J, Guo W, Chen J, Liang S, Qian W and Yuan X. Usage of Yb(OH)CO3 nanoparticles-based computed tomography image in the prediction model of lung biopsy pneumothorax. Cell Mol Biol (Noisy-le-grand) 2022; 68: 258-269.
[37] Hu W, Ying Y, Jin L, Chen L, Zhou T and Jin X. PMN apoptosis induced by SNHG11 through the inhibition of endotoxin-induced acute lung injury NF-κB pathway. Cell Mol Biol (Noisy-le-grand) 2022; 68: 145-152.
[38] Ren X, Luo T, Ma H, Zhou M and Yu S. Immunotherapy and prognosis of non-small cell lung carcinoma by monomethoxy polyethylene glycol-hyaluronic acid-platinum combined with immune CT4+ and CT8+ detection. Cell Mol Biol (Noisy-le-grand) 2022; 68: 167-173.
[39] Ma M, Wang W, Wang B, Yang Y, Huang Y, Zhao G and Ye L. The prognostic value of N6-methyladenosine RBM15 regulators in lung adenocarcinoma. Cell Mol Biol (Noisy-le-grand) 2022; 68: 130-139.
[40] Lei L and Weidong Z. Small molecule TKI inhibitors affect the development of non-small cell carcinoma through HIPPO/YAP/PD-L1. Cell Mol Biol (Noisy-le-grand) 2022; 67: 117-122.
[41] Chen J, Li D, Huang Z, Zheng C, Lin Q, Feng N, Chen S and Cao X. Role of mitophagy-based TLR9 signal pathway in neonatal ventilator-induced lung injury. Cell Mol Biol (Noisy-le-grand) 2022; 68: 103-110.
[42] Sha Y, Wang J, Wang Z, Zhang X and Chen J. Analysis of the effect of a new type of nano-drug carrier preparation on the pathological changes in lung and inducible nitric-oxide synthase expression in severe sepsis. Cell Mol Biol (Noisy-le-grand) 2022; 68: 1-7.
[43] Li Y, Xiong J and Ye W. Analysis of macrophage chemotactic activity and TLR9 signaling pathway in the mouse model of viral acute lung injury. Cell Mol Biol (Noisy-le-grand) 2022; 68: 71-7.
[44] Bai Y, Wang X and Zhang J. The effect of thoracic epidural nerve block with dezocine and ropivacaine on arterial oxygen saturation and IDO gene expression during pulmonary ventilation in lung resection surgery. Cell Mol Biol (Noisy-le-grand) 2022; 68: 25-30.
[45] Kang H, Chen J and Cao S. Propofol regulates the expression of BecliN-1 through miR-30b and protects against lung ischemia-reperfusion injury. Cell Mol Biol (Noisy-le-grand) 2022; 67: 348-355.
[46] Zhang Y, Zhang J, Wang M and Zhao T. Repairing effect of new dexamethasone nanoparticles in the treatment of acute lung injury and cluster nursing. Cell Mol Biol (Noisy-le-grand) 2022; 68: 140-148.
[47] Behzadmehr R and Rezaie-Keikhaie K. Evaluation of active pulmonary tuberculosis among women with diabetes. Cell Mol Biomed Rep 2022; 2: 56-63.
[48] Rezaie-Kahkhaie K, Rezaie-Keikhaie K, Rezaie-Kahkhaie L, Saravani K and kamali A. The relationship between IL23R 1142G/A (Arg381Gln) and GM-CSF 3928 C/T (Ile117Thr) gene polymorphism in Iranian patients with tuberculosis disease. Cell Mol Biomed Rep 2021; 1: 113-121.